Journal of Zhejiang University-SCIENCE B (Biomedicine & Biotechnology)
ISSN 1673-1581 (Print); ISSN 1862-1783 (Online)
www.jzus.zju.edu.cn; www.springerlink.com
E-mail: jzus@zju.edu.cn

MiR-1180 from bone marrow-derived mesenchymal stem cells induces glycolysis and chemoresistance in ovarian cancer cells by upregulating the Wnt signaling pathway*

Zhuo-wei GU[1,2], Yi-feng HE[†‡1,2], Wen-jing WANG[1,2], Qi TIAN[1,2], Wen DI[†‡1,2]

[1]*Department of Obstetrics and Gynecology, Ren Ji Hospital, School of Medicine, Shanghai Jiao Tong University, Shanghai 200127, China*

[2]*Shanghai Key Laboratory of Gynecologic Oncology, Ren Ji Hospital, School of Medicine, Shanghai Jiao Tong University, Shanghai 200127, China*

[†]E-mail: he_yifeng@hotmail.com; diwen163@163.com

Received Mar. 29, 2018; Revision accepted Dec. 11, 2018; Crosschecked Jan. 9, 2019

Abstract: Background: Bone marrow-derived mesenchymal stem cells (BM-MSCs) play an important role in cancer development and progression. However, the mechanism by which they enhance the chemoresistance of ovarian cancer is unknown. Methods: Conditioned media of BM-MSCs (BM-MSC-CM) were analyzed using a technique based on microRNA arrays. The most highly expressed microRNAs were selected for testing their effects on glycolysis and chemoresistance in SKOV3 and COC1 ovarian cancer cells. The targeted gene and related signaling pathway were investigated using in silico analysis and in vitro cancer cell models. Kaplan-Merier survival analysis was performed on a population of 59 patients enrolled to analyze the clinical significance of microRNA findings in the prognosis of ovarian cancer. Results: MiR-1180 was the most abundant microRNA detected in BM-MSC-CM, which simultaneously induces glycolysis and chemoresistance (against cisplatin) in ovarian cancer cells. The secreted frizzled-related protein 1 (*SFRP1*) gene was identified as a major target of miR-1180. The overexpression of miR-1180 led to the activation of Wnt signaling and its downstream components, namely Wnt5a, β-catenin, c-Myc, and CyclinD1, which are responsible for glycolysis-induced chemoresistance. The miR-1180 level was inversely correlated with *SFRP1* mRNA expression in ovarian cancer tissue. The overexpressed miR-1180 was associated with a poor prognosis for the long-term (96-month) survival of ovarian cancer patients. Conclusions: BM-MSCs enhance the chemoresistance of ovarian cancer by releasing miR-1180. The released miR-1180 activates the Wnt signaling pathway in cancer cells by targeting *SFRP1*. The enhanced Wnt signaling upregulates the glycolytic level (i.e. Warburg effect), which reinforces the chemoresistance property of ovarian cancer cells.

Key words: Chemoresistant ovarian cancer; Mesenchymal stem cell; MiR-1180; Secreted frizzled-related protein 1 (SFRP1); Wnt; Glycolysis
https://doi.org/10.1631/jzus.B1800190 **CLC number:** R737.31

1 Introduction

Mesenchymal stem cells (MSCs) are self-renewal multipotent progenitors that inhabit the stromal compartment (Vallabhaneni et al., 2016; Ridge et al., 2017). The stem cells isolated from bone marrow (BM) stroma that have the potential to differentiate into diverse mesenchymal tissues, such as adipose, cartilage, and muscle, are known as bone

‡ Corresponding authors
* Project supported by the National Key Research and Development Program of China (No. 2016YFC1303100), the Science and Technology Commission of Shanghai Municipality (Nos. 15441905700, 15DZ1940502, and 12411950200), the Shanghai Municipal Commission of Health and Family Planning (No. 2013ZYJB0202), and the National Natural Science Foundation of China (Nos. 81572548, 81772770, 81272882, and 81072137)
ORCID: Zhuo-wei GU, https://orcid.org/0000-0002-7357-6364; Yi-feng HE, https://orcid.org/0000-0003-0764-8806; Wen DI, https://orcid.org/0000-0003-4007-3856

marrow-derived mesenchymal stem cells (BM-MSCs) (Huang et al., 2014; Tyciakova et al., 2015; Wang et al., 2015; Yang et al., 2015; Watts et al., 2016; Fu et al., 2017; Xiang et al., 2017). Circulating BM-MSCs can support cancer development via intercellular communication molecules, such as cytokines and exosome-delivered microRNAs, which induce immune tolerance, epithelial-to-mesenchymal transition of cancer cells and angiogenesis in the local microenvironment (McLean et al., 2011; Castells et al., 2013; Touboul et al., 2013; Lis et al., 2014; Coffman et al., 2016). In gynecological oncology, ovarian cancer is a frequently encountered malignancy with the highest mortality. Uncontrollable cancer growth and metastasis caused by chemoresistance is a major cause of death in ovarian cancer. The role of MSCs, including BM-MSCs, in the progression of ovarian cancer, has been investigated (Mader et al., 2009; Lis et al., 2011; Touboul et al., 2014). Some intrinsic biochemical factors, such as glycolysis-induced lactic acidosis, were found to be involved in the chemoresistance mechanisms. However, as extrinsic biochemical factors, the effects of BM-MSCs and their derived microRNAs on the development of chemoresistance in ovarian cancer remain unclear.

The importance of glycolysis or the so-called "Warburg effect" on the occurrence of chemoresistance in cancer cells has been documented by Wu et al. (2012). They demonstrated that glycolysis-induced lactic acidosis, but not glycolysis-related lactosis or acidosis, enhances the expression of Bcl-2 and phosphorylation of Akt, and suppresses the function of the mammalian target of rapamycin (mTOR), thereby enabling the cancer cells to survive under unfavorable and stringent growth conditions (Wu et al., 2012). Since glycolysis-induced lactic acidosis is widely accepted as an intrinsic factor that can induce chemoresistance in a variety of malignancies (Ganapathy-Kanniappan and Geschwind, 2013; Suh et al., 2014; Icard et al., 2018; Yao K et al., 2018), in this study, we hypothesized that BM-MSCs, particularly their derived microRNAs, could influence intracellular glycolysis and enhance the chemoresistance of ovarian cancer. Based on supportive data obtained from our in vitro cancer cell models, we investigated the exact microRNA molecule(s) released by BM-MSCs that induced the glycolysis-related chemoresistance in ovarian cancer cells. MiR-1180 was identified as a key communication molecule for BM-MSCs to control intracellular glycolysis, while a secreted frizzled-related protein 1 (SFRP1)/Wnt signaling pathway-based mechanism was found to be responsible for the observed effect of miR-1180 in the investigated cancer cells. Our results suggest that BM-MSC-derived miR-1180 could be a novel therapeutic target for reversing the chemoresistance of ovarian cancer.

2 Materials and methods

2.1 Study population

Surgical specimens and medical records were collected from 59 ovarian cancer patients enrolled at Ren Ji Hospital, School of Medicine, Shanghai Jiao Tong University (Shanghai, China) from Mar. 1, 2008 to Jan. 1, 2009. Chemoresistant recurrence was defined as a recurrence event emerging within six months after a regular course of chemotherapy. All the patients were followed up from their initial surgical and/or chemical treatments until death. The duration of follow-up ranged from 5 to 96 months. Informed consent was obtained from each patient, and the study protocol was approved by the ethics committee of Ren Ji Hospital.

2.2 Cell cultures

The ovarian cancer cell lines SKOV3 and COC1 and the normal ovarian epithelial cell line IOSE80 were purchased from the American Type Culture Collection (ATCC, Manassas, VA, USA). Cells were cultured in Dulbecco's modified Eagle's medium/Ham's F-12 medium (DMEM/F12; Gibco, Life Technologies, Grand Island, NY, USA) supplemented with 10% fetal bovine serum (FBS; Gibco), penicillin (Gibco), and streptomycin (Gibco) in a humidified incubator with 5% CO_2 at 37 °C. For IOSE80 cells, 100 ng/mL epidermal growth factor (EGF; Sigma-Aldrich, St. Louis, MO, USA) and 10 nmol/L insulin (Sigma) were supplemented.

2.3 Preparation of conditioned medium

The primary BM-MSCs were purchased from the Shanghai Bangjing Biotechnology Co. (Shanghai, China). The cells were collected from a Stage IIIc ovarian cancer patient with chemoresistant recurrence

within six months after chemotherapy (informed consent was obtained). The BM-MSCs were cultured in DMEM/F12 (Gibco, glucose=1 g/L) supplemented with 10% FBS (microRNA-free, exosome-deleted, Gibco) for 24 h. Conditioned medium (CM) was collected and filtered with a 0.22-μm filter (Merck Millipore, MA, USA) to remove cell debris.

2.4 Cell proliferation assay

Cells were cultured in 96-well plates and the number of cells was measured using the 3-(4,5-dimethylthiazol-2-yl)-2,5-diphenyltetrazolium bromide (MTT) method. For MTT assays, phenol red-free medium-dissolved MTT (Sigma) was added to each well to a final concentration of 1 mg/mL. Following a 4-h incubation, the medium in each well was replaced with 100 μL of dimethyl sulfoxide. The plate was then covered with tinfoil and agitated on an orbital shaker for 15 min. Absorbance was recorded at 570 nm with a filter reference at 620 nm using a Varioskan Flash Multimode Plate Reader (Thermo Fisher Scientific, Waltham, MA, USA). The number of the measured cells was estimated based on the MTT optical density (OD)-cell number standard curve.

2.5 Clonogenic assay

The saline control or cisplatin-treated cells were seeded in 6-well plates. Their survival rates were determined by a modified clonogenic assay according to methods described previously (He et al., 2016). The colonies (>50 cells) formed at a given cisplatin concentration (treated for 24 h) were allowed to grow for 10 d in normal media (DMEM/F12 supplemented with 10% FBS) and were then counted using a stereoscope.

2.6 ECAR measurement

Extracellular acidification rate (ECAR) measurements were performed using an XF24 or XF96 Extracellular Flux analyzer (Seahorse Bioscience, North Billerica, MA, USA) as described by Wu et al. (2007). To determine the baseline ECAR, cells were initially cultured in a glucose/L-glutamine/pyruvate/phenol red-free DMEM (Gibco) for 24 h in 5% CO_2 at 37 °C. The medium was then changed to normal DMEM/F12 or BM-MSC-CM, in which the glucose concentration was adjusted to 2 g/L, to measure actual ECARs. The ECAR value corresponding to the cells following the 2 mg/mL oligomycin (Sigma) blockade of mitochondrial energy metabolism represented a maximal glycolytic capacity. 2-Deoxy-D-glucose (2-DG) at a final concentration of 100 mmol/L was used for abolishing the observed intracellular glycolysis.

2.7 ATP assay

The adenosine triphosphate (ATP) concentration within the cultured cells was assessed using a colorimetric ATP Assay Kit (Abcam, Cambridge, UK). Whole-cell extracts of equal numbers of cancer cells from normal media and from BM-MSC-CM were applied for each comparative experiment.

2.8 MicroRNA array, anti-sense microRNA, and microRNA mimics

The miRCURY Exosome Kit (Qiagen, Venlo, The Netherlands) was used for isolating BM-MSC-derived exosomes from the conditioned media. Exosome-delivered microRNA was isolated with the miRNeasy Micro Kit (Qiagen). The Affymetrix GeneChip miRNA 4.0 Array was used for profiling the microRNAs released by BM-MSCs. The anti-sense sequence and mimics of miR-1180 were purchased from Qiagen.

2.9 RT-qPCR

Intracellular mRNA was isolated using TRIzol reagent (Thermo Fisher Scientific) and then reverse-transcribed using a Universal cDNA Synthesis Kit (Exiqon, Vedbaek, Denmark). The primers used for amplifying (precursor) microRNAs and *SFRP1*-encoding cDNA in reverse transcription-quantitative polymerase chain reaction (RT-qPCR) were all purchased from Qiagen. SYBR Green I dye (Thermo Fisher Scientific) served as a quantitative indicator in the qPCR reaction. An ABI PRISM 7900 Sequence Detection System (Applied Biosystems, Carlsbad, CA, USA) was used for PCR amplification. The *U6* small nuclear RNAs (snRNA) and *β-actin* mRNA levels were set as the references for microRNA and mRNA quantification. The relative expression levels of pre-miR-1180/miR-1180 and *SFRP1* were calculated using the $2^{-\Delta\Delta C_T}$ method. The T-N value was calculated as the miR-1180 level of cancer tissue minus the miR-1180 level of adjacent normal tissue. The baseline level of pre-miR-1180 was determined by an average level of this molecule expressed in the adjacent normal tissue of the enrolled patients.

2.10 Luciferase reporter assay

The wide-type (5'-UGCCCCGGGAACCCGGUGGGUCA-3') and mutant (5'-UGCCCCGGGAACCCGGUUUUUCA-3') 3' untranslated region (UTR) sequences of the *SFRP1* gene were synthesized (Sangon, Shanghai, China) and inserted into the multiple cloning site of a luciferase reporter plasmid pMIR-REPORT (Thermo Fisher Scientific). Luciferase activity was measured using a Pierce Firefly Luciferase Glow Assay Kit (Thermo Fisher Scientific) according to the manufacturer's instructions. Luciferase activity of the control microRNA-treated cells was set as 1.

2.11 Western blotting

Cells were harvested and lysed with radioimmunoprecipitation assay (RIPA) buffer containing protease inhibitors (Thermo Fisher Scientific) on ice for 30 min. Proteins were separated by 10% (0.1 g/mL) sodium dodecyl sulfate-polyacrylamide gel electrophoresis (SDS-PAGE; Thermo Fisher Scientific). The proteins were transferred onto nitrocellulose membranes and probed with primary antibodies and then horseradish peroxidase-labeled secondary antibodies (Thermo Fisher Scientific). The protein band signals were visualized using an enhanced chemiluminescence (ECL; Thermo Fisher Scientific). The primary antibodies were rabbit anti-human LDHA monoclonal antibody (1:1000, clone EPR1564, Abcam), mouse anti-human HK2 monoclonal antibody (1:500, clone 3D3, Abcam), mouse anti-human PDK1 monoclonal antibody (1:500, clone 4A11, Abcam), rabbit anti-human PKM2 polyclonal antibody (1:500, product No. ab137852, Abcam), rabbit anti-human SFRP1 monoclonal antibody (1:1000, clone EPR7003, Abcam), rabbit anti-human Wnt5a monoclonal antibody (1:1000, clone EPR12698, Abcam), rabbit anti-human β-catenin monoclonal antibody (1:1000, clone E247, Abcam), rabbit anti-human c-Myc monoclonal antibody (1:1000, clone Y69, Abcam), and rabbit anti-human CyclinD1 monoclonal antibody (1:1000, clone EP272Y, Abcam). The secondary antibodies, IRDye 680RD goat anti-mouse IgG (1:10000, LI-COR, Lincoln, NE, USA) and IRDye 800CW goat anti-rabbit IgG (1:10000, LI-COR), were used as appropriate. The western blotting bands were visualized using a C-DiGit Blot Scanner (LI-COR).

2.12 Fluorescence-activated cell sorting

Cells were suspended in an FcR blocking reagent (Miltenyi Biotec, Bergisch Gladbach, Germany) containing 5% phosphate-buffered saline (PBS), 1% FBS, and 10% bovine serum albumin (BSA). Single-cell suspensions were analyzed and sorted on a MoFlo XDP cell sorter (Beckman Coulter, Brea, CA, USA). PE-conjugated mouse anti-human CD271 monoclonal antibody (1:25; clone NGFR5, Abcam) was used for labeling BM-MSCs, and Alexa Fluor 488-conjugated mouse anti-human EpCAM monoclonal antibody (1:50; clone VU1D9, Cell Signaling, Carlsbad, CA, USA) for labeling ovarian cancer cells. Note that CD271, also called p75 neurotrophin receptor, is widely recognized as a marker of MSCs (Quirici et al., 2002; Das et al., 2013; Rasini et al., 2013; Watson et al., 2013), especially BM-MSCs (Jones et al., 2008; Noort et al., 2012).

2.13 Immunohistochemistry

Immunohistochemistry (IHC) was performed to verify the flow-cytometry/fluorescence-activated cell sorting (FACS) results of CD271-positive or EpCAM-positive cells in the specimens. As described previously (Zhang et al., 2014), the cancer specimens were sliced into 4-μm sections, dewaxed using xylene, and rehydrated with graduated ethanol. Antigen retrieval was performed using a microwave at >90 °C for 15 min, and the samples were allowed to cool to room temperature. The non-specific binding sites were blocked with 5% BSA for 1 h. The antibody-binding sites were visualized using 3,3'-diaminobenzidine tetrahydrochloride (DAB; Zhongshan, Beijing, China), and the cell nuclei were counterstained with hematoxylin.

2.14 Statistical analysis

Two-sided Student's *t*-tests were used for numerical data and χ^2-test/Fisher's exact tests for nominal data. Kaplan-Meier analysis was used to compare 96-month overall survival between the patients with higher (>median) and lower (≤median) expression of miR-1180. A Cox regression model was used for multivariate analysis on the prognostic factors for long-term outcomes and chemoresistance of the patients. Pearson's product-moment correlation coefficient analysis was used for evaluating the relationship between intra-tumoral miR-1180 and SFRP1 expression

levels. All statistical analyses were carried out using SPSS 18.0 software (SPSS, Chicago, IL, USA). Unless otherwise indicated, all experiments were performed in triplicate. P values of <0.05 were considered statistically significant.

3 Results

3.1 Effect of BM-MSC-CM on the chemoresistant property of in vitro cultured ovarian cancer cells

To investigate the role of BM-MSCs, particularly the BM-MSC-CM, in the chemoresistant behavior of ovarian cancer cells, SKOV3 and COC1 cells were cultured in the BM-MSC-CM for 24 h. Their proliferative curves were measured by the MTT method during the following five days. The obtained data indicated that the addition of BM-MSC-CM accelerated the proliferation of SKOV3 and COC1 cells (Fig. 1a). When cisplatin was administered into the cell cultures at a final concentration of 0.5 mg/L for 24 h and then substituted with normal media, the cells pretreated with the BM-MSC-CM exhibited a significantly higher proliferative rate than control cells (Fig. 1a). The anti-cisplatin effects of BM-MSC-CM on SKOV3 and COC1 cells were revealed by clonogenic assays. The addition of BM-MSC-CM significantly promoted colony formation by cancer cells under a non-cisplatin culture condition as well as under a cisplatin-containing condition (Fig. 1b).

3.2 Effect of BM-MSC-CM on glycolysis in cultured ovarian cancer cells

To evaluate the effect of BM-MSC-CM on the glycolytic status of ovarian cancer cells, we measured the ECARs in SKOV3 and COC1 cells treated with or without BM-MSC-CM. Remarkable increases were observed in the ECARs of BM-MSC-CM-treated SKOV3 and COC1 cells (Fig. 2a). Furthermore, the treatment with 0.5 mg/mL oligomycin, an inducer of glycolysis and an inhibitor of mitochondrial oxidative phosphorylation, revealed that BM-MSC-CM-treated cells had a significantly increased glycolytic capacity compared to their normal medium-treated counterparts (Fig. 2a). ATP production in both SKOV3 and COC1 cells increased after BM-MSC-CM treatment (Fig. 2b). Correspondingly, expression levels of the key glycolytic enzymes LDHA, HK2, PDK1, and PKM2 were all upregulated when BM-MSC-CM was applied (Fig. 2b). These data suggest that BM-MSCs can influence the intracellular glycolysis of cancer cells via a remote communication approach (i.e. endocrine or paracrine). Next, to verify the chemoresistance-promoting effect of glycolysis, we treated the SKOV3 and COC1 cells with oligomycin and recorded their proliferative and colony formation behaviors in a cisplatin-containing condition. The ECARs of both cell lines were significantly increased upon the addition of oligomycin (Fig. 2a) and their proliferation rates and colony formation abilities were significantly higher than those of the controls treated with cisplatin at 0.5 mg/L for 24 h and then in normal media (Fig. 2c). These results suggest that glycolysis is a necessary mediator of BM-MSC-CM-induced chemoresistance.

3.3 Up-regulation of miR-1180 level in the BM-MSC-CM

To explore the possible microRNA-based mechanism of BM-MSCs in remote regulation of glycolysis of ovarian cancer cells, we profiled the exosome-associated microRNAs in BM-MSC-CM via an exosome-harvesting-based miRNA array analysis (see Section 2). The results are shown in Fig. 3a. Three microRNAs, namely miR-1180, miR-628-5p, and miR-432-5p, were most highly expressed in BM-MSC-CM, while another microRNA, miR-2114, was found to be at the lowest level compared with the control CM derived from the IOSE80 cell line. These four microRNAs were subjected to RT-qPCR analysis. The quantification results verified that miR-1180 ((8.2±0.5) folds), miR-628-5p ((6.2±0.7) folds), and miR-432-5p ((5.3±0.3) folds) were significantly upregulated in BM-MSC-CM while miR-2114 ((0.46±0.06) folds) was significantly downregulated (Figs. 3b–3e). Further parallel RT-qPCR analyses in SKOV3 and COC1 cells revealed that miR-1180 expression was much lowered in SKOV3 cells and almost absent in COC1 cells compared with the BM-MSCs (Fig. 3b). MiR-628-5p, miR-432-5p, and miR-2114 molecules were found to be moderately expressed in at least one of the cancer cell lines tested (Figs. 3c–3e). Therefore, only the most abundantly expressed microRNA, miR-1180, can be a possible signaling molecule that induces glycolysis enhancement in both cancer cell lines. Thus, molecule miR-1180 was selected for further investigation of its exact function.

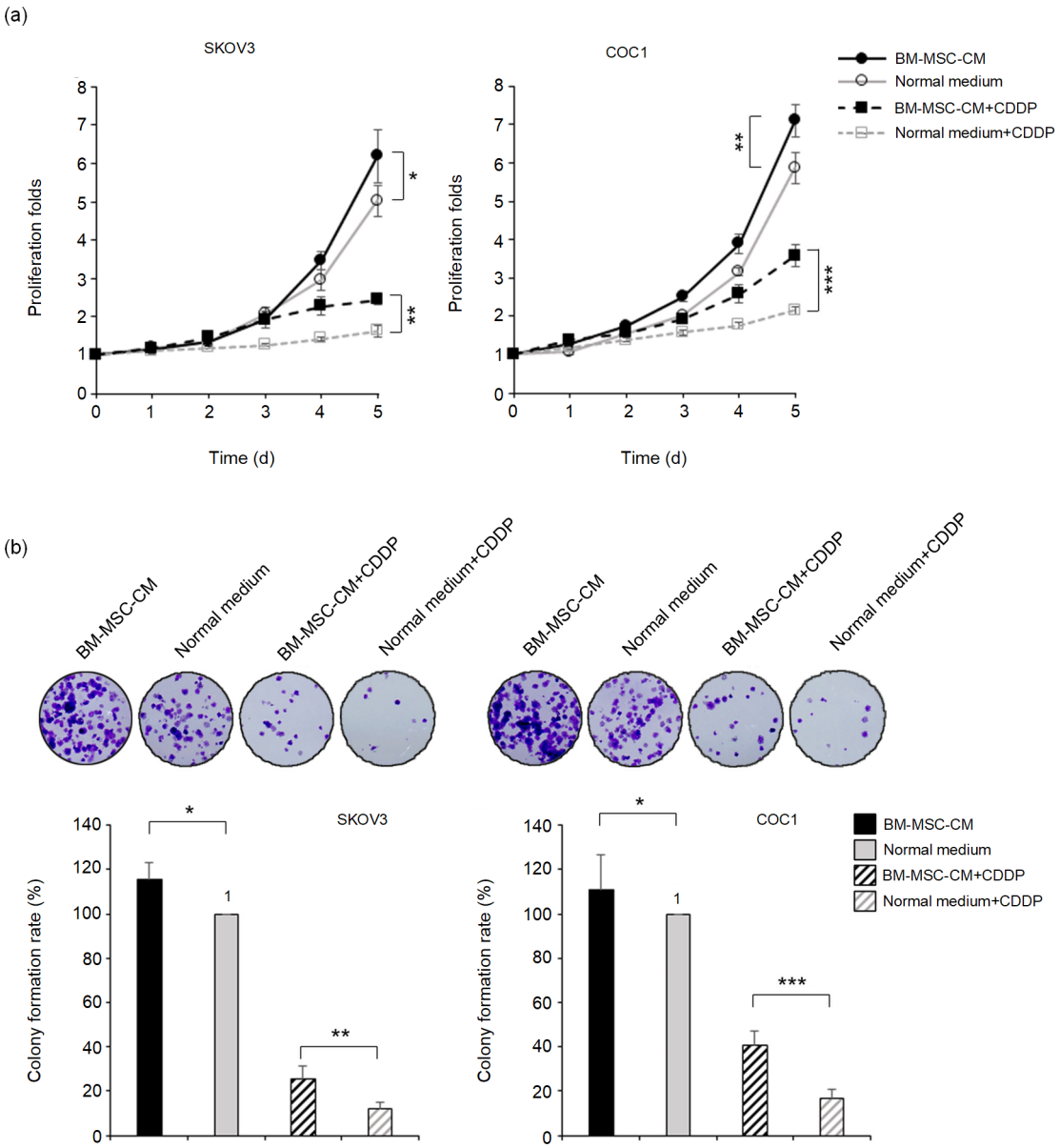

Fig. 1 Enhancement of BM-MSC-CM on the chemoresistance of ovarian cancer cells

(a) Proliferative curves for SKOV3 and COC1 ovarian cancer cells treated with or without BM-MSC-CM under a normal or a cisplatin-containing condition (0.5 mg/L, for 24 h). (b) Colony formation abilities of SKOV3 and COC1 cells treated with or without BM-MSC-CM under a normal or a cisplatin-containing condition (0.5 mg/L). * P<0.05, ** P<0.01, *** P<0.001, two-sided Student's t-test. Data are expressed as mean±standard deviation (SD). CDDP: *cis*-Dichlorodiammine platinum (II)

3.4 Effect of miR-1180 knockdown on the regulation of BM-MSC-CM on glycolysis in ovarian cancer cells

The role of BM-MSC-derived miR-1180 in the regulation of cancer cell glycolysis was investigated using an antisense microRNA-based technique. The synthesized anti-miR-1180 effectively decreased the secretory level of miR-1180 in the BM-MSC-CM (Fig. 4a). The proliferative curves of BM-MSC-CM-treated SKOV3 and COC1 cells were downregulated in a cisplatin-containing (0.5 mg/L) condition after miR-1180 knockdown (Fig. 4b). Correspondingly, their colony formation abilities were reduced by these treatments (Fig. 4c). To evaluate the influence of miR-1180 knockdown on ovarian cancer cell glycolysis, the ECARs of cancer cells treated with either miR-1180-deprived BM-MSC-CM or normal BM-MSC-CM were compared. The anti-miR-1180

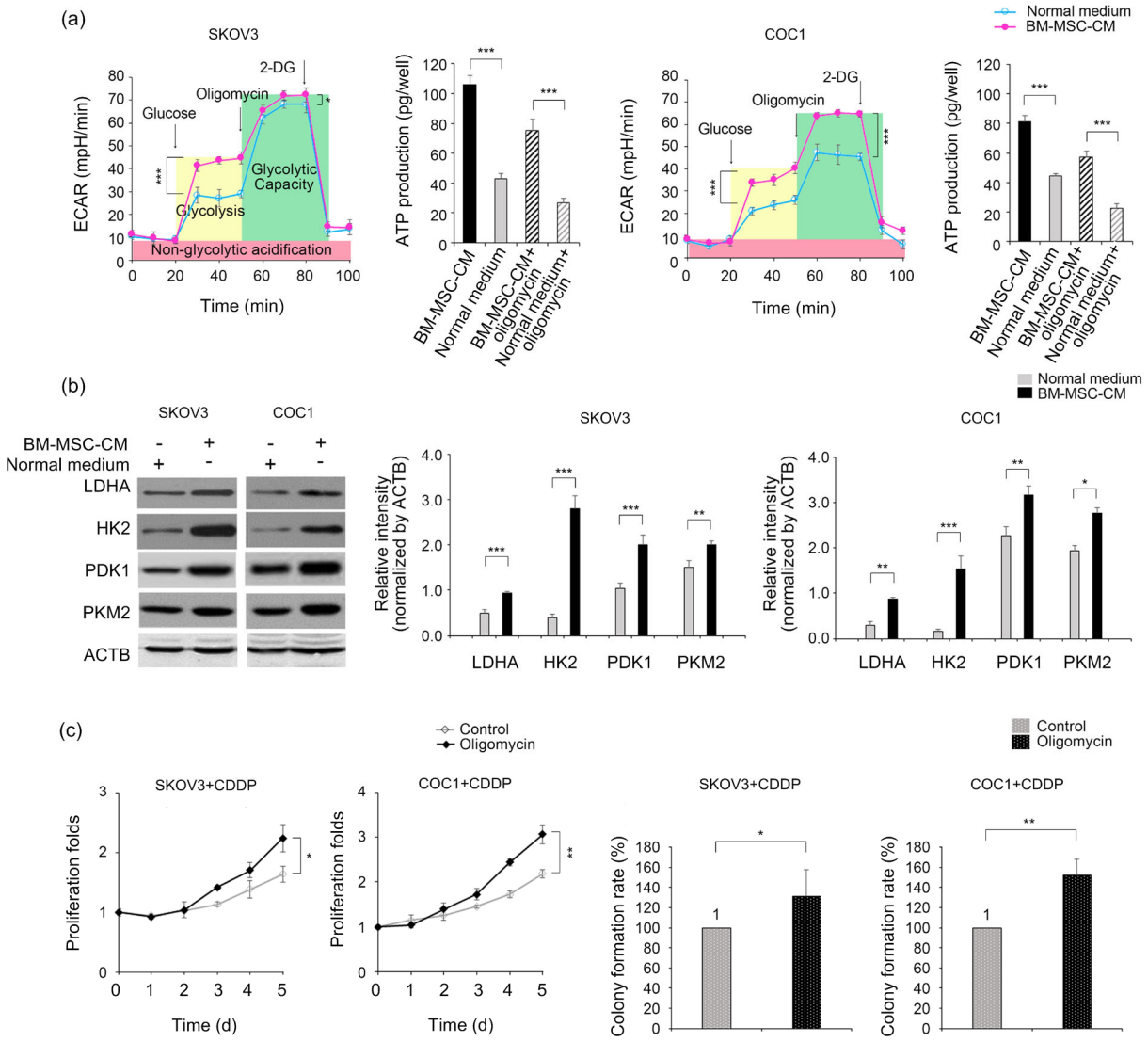

Fig. 2 Promotion of BM-MSC-CM on the glycolysis of ovarian cancer cells

(a) ECARs of SKOV3 and COC1 cells treated with or without BM-MSC-CM for 24 h. Cells were cultured in glucose/L-glutamine/pyruvate/phenol red-free DMEM or BM-MSC-CM. To activate intracellular glycolysis, glucose (at a final concentration of 2 g/L) was supplemented. To test the maximal capacity of glycolysis, oligomycin (2 mg/mL) was applied. Glycolysis was ceased by an addition of 2-DG. ATP production was measured in the cells before and after being challenged with oligomycin, with or without a BM-MSC-CM pre-treatment (for 24 h). (b) Western blotting analysis of the key enzymes of glycolysis in cells cultured in a normal medium or in BM-MSC-CM. (c) Proliferative curves and colony formation rates for oligomycin-treated cancer cells under a cisplatin-containing condition. * $P<0.05$, ** $P<0.01$, *** $P<0.001$, two-sided Student's t-test. Data are expressed as mean±standard deviation (SD)

significantly reduced ECARs in the BM-MSC-CM-treated SKOV3 and COC1 cells, implying a critical role of miR-1180 in BM-MSC-induced glycolysis (Fig. 4d). Likewise, ATP production was significantly suppressed in SKOV3 and COC1 cells in miR-1180-deprived BM-MSC-CM compared with those in normal BM-MSC-CM (Fig. 4e).

3.5 Effect of BM-MSC-derived miR-1180 on the expression of SFRP1 and the Wnt signaling pathway

We used the microRNA target gene prediction software Targetscan to search for a potential intracellular signaling element between miR-1180 and its cytological effect on glycolysis. Since the Wnt

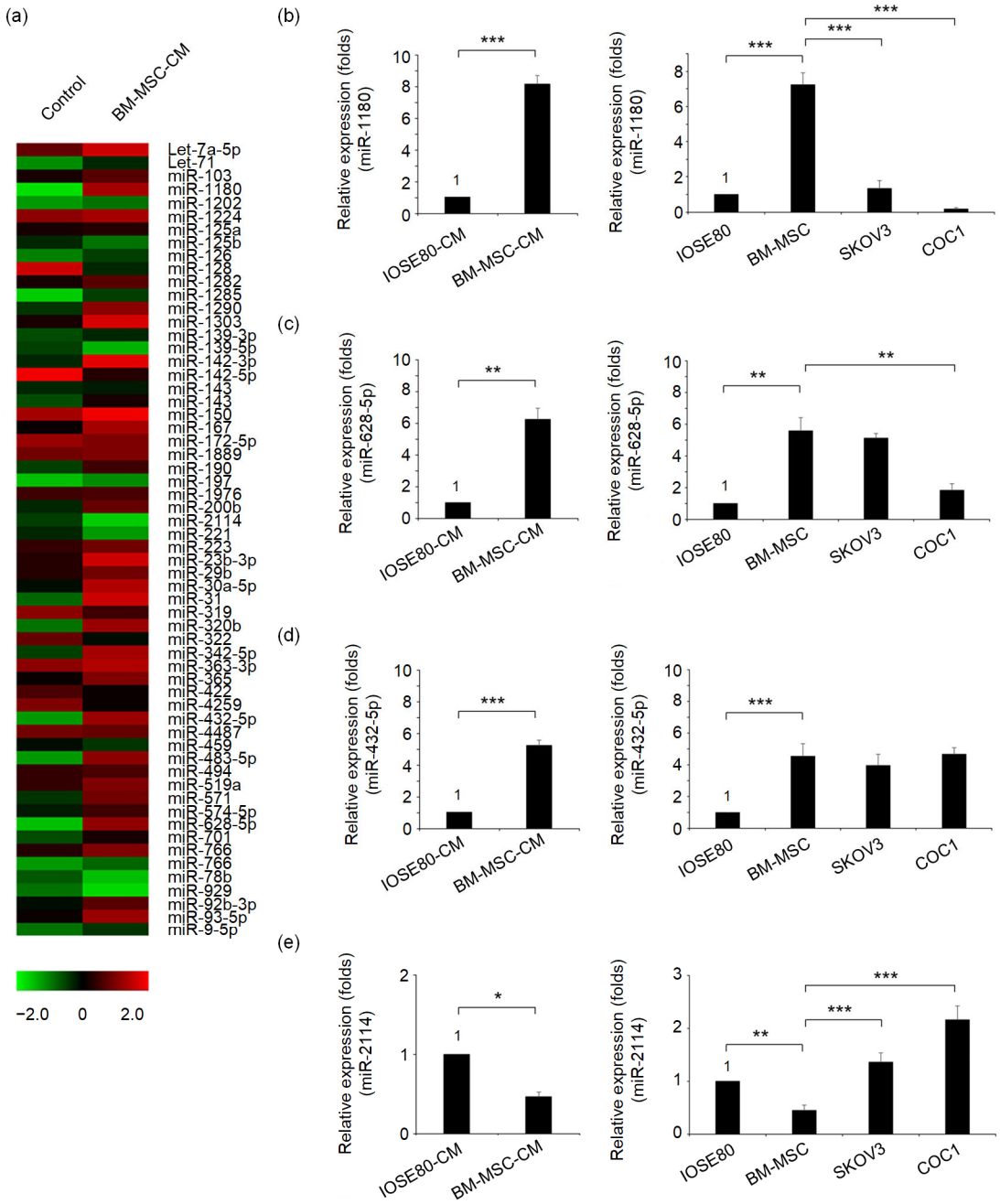

Fig. 3 Expression profile of BM-MSC-CM-derived microRNAs

(a) A heat map of the microRNA profiling data obtained from the negative control (i.e. IOSE80-CM) and BM-MSC-CM. (b–e) Comparisons of the microRNA qPCR data from IOSE80-CM and BM-MSC-CM, and those from IOSE80, BM-MSCs, SKOV3 and COC1 cells (for microRNA intracellular levels) for miR-1180 (b), miR-628-5p (c), miR-432-5p (d), and miR-2114 (e). * P<0.05, ** P<0.01, *** P<0.001, two-sided Student's t-test. Data are expressed as mean±standard deviation (SD)

signaling pathway has been confirmed by previous studies to be involved in the glycolysis-regulatory mechanism (Pate et al., 2014), SFRP1, a negative regulator of the Wnt signaling pathway (Arend et al., 2013), was identified as a most likely target gene for miR-1180. Therefore, we built luciferase reporter plasmids that harbor the wild-type (WT) or mutant (Mut) 3' UTR sequences of SFRP1 to verify the direct binding of miR-1180 to the SFRP1 mRNA (Fig. 5a). The luciferase activity of SFRP1 WT-3' UTR-encoding plasmids in the SKOV3 and COC1 cells (Fig. 5b) was reduced to 51% (SKOV3) and 43% (COC1) of

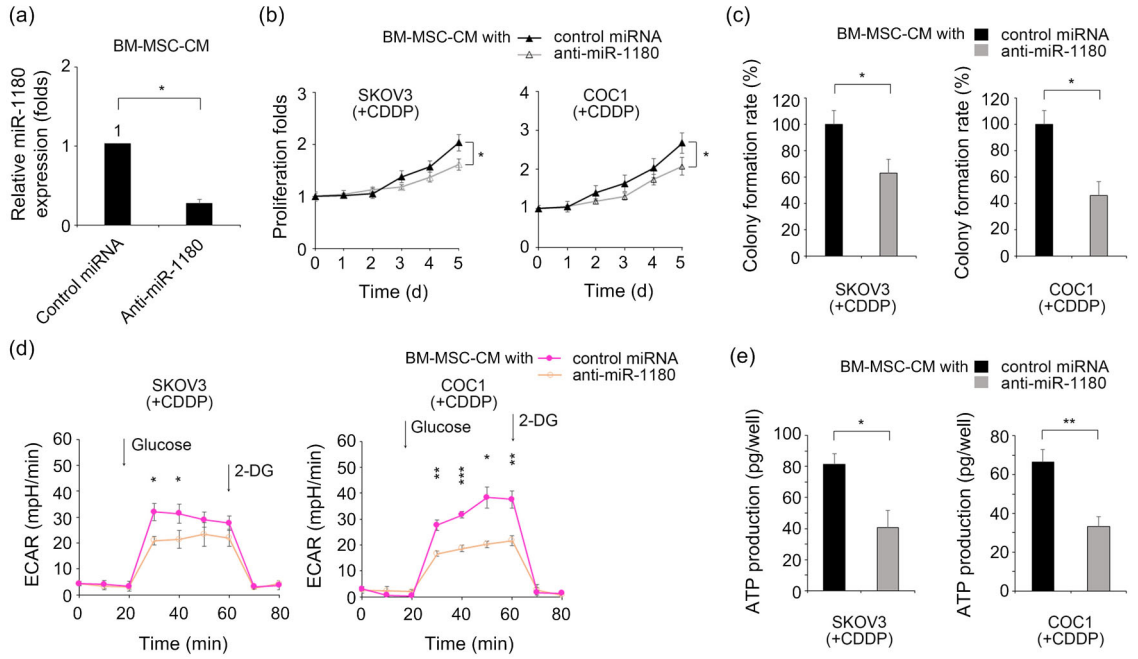

Fig. 4 Enhancement of BM-MSC-CM-derived miR-1180 on the glycolysis and chemoresistance of ovarian cancer cells
(a) Comparison of miR-1180 levels in control microRNA- or anti-miR-1180-supplemented BM-MSC-CM. (b) Proliferative curves of SKOV3 and COC1 cells in normal or miR-1180-deprived BM-MSC-CM under a cisplatin-containing condition (0.5 mg/L). (c) Colony formation abilities of SKOV3 and COC1 cells in normal or miR-1180-deprived BM-MSC-CM under a cisplatin-containing condition (0.5 mg/L). (d) The ECARs of SKOV3 and COC1 cells in normal medium or miR-1180-deprived BM-MSC-CM under a cisplatin-containing condition (0.5 mg/L). (e) ATP production of SKOV3 and COC1 cells in normal or miR-1180-deprived BM-MSC-CM under a cisplatin-containing condition (0.5 mg/L). * P<0.05, ** P<0.01, *** P<0.001, two-sided Student's t-test. Data are expressed as mean±standard deviation (SD)

those observed in corresponding control-microRNA-treated cells after the addition of miR-1180 mimics. However, no inhibitory effect was found on the luciferase activity of SFRP1 Mut-3' UTR-encoding plasmid in these cells (Fig. 5b).

Both the mRNA and protein levels of SFRP1 were downregulated in SKOV3 and COC1 cells after the addition of miR-1180 mimics (Figs. 5c and 5d). The same expression regulatory patterns in SFRP1 were observed when BM-MSC-CM was added, demonstrating that miR-1180 is a major mediator of BM-MSC-CM in controlling the expression of SFRP1 (Fig. 5c). Furthermore, the expression levels of the corresponding Wnt signaling effector proteins Wnt5a, β-catenin, c-Myc, and CyclinD1 were significantly upregulated after transfection of miR-1180 mimics or treatment with BM-MSC-CM (Fig. 5c). The proliferation rates, colony formation abilities, and ECARs of both cell lines were elevated following a 24-h miR-1180 treatment under either a normal or a cisplatin-containing culture condition (Figs. 5e–5g), while the forced expression of SFRP1 (achieved by transfection of an SFRP1 cDNA-encoding plasmid), even in the presence of miR-1180, resulted in decreased activity of the Wnt signaling pathway (Fig. 5c), implying its potential as a tool to reverse the chemoresistance of ovarian cancer.

3.6 Correlations of elevated expression of miR-1180 with poor prognosis and SFRP1 expression in ovarian cancer tissue

The clinical implications of miR-1180 overexpression were explored in the 59 enrolled ovarian cancer patients (Fig. 6a and Table 1). The miR-1180 levels in the tumor mass and adjacent normal tissue were compared for each patient (presented as T-N values). In most (42/59) cases, the detected miR-1180 levels (normalized by U6 snRNA) were higher in the tumor mass than in normal tissue (Fig. 6a). The average expression level of intra-tumoral miR-1180 was

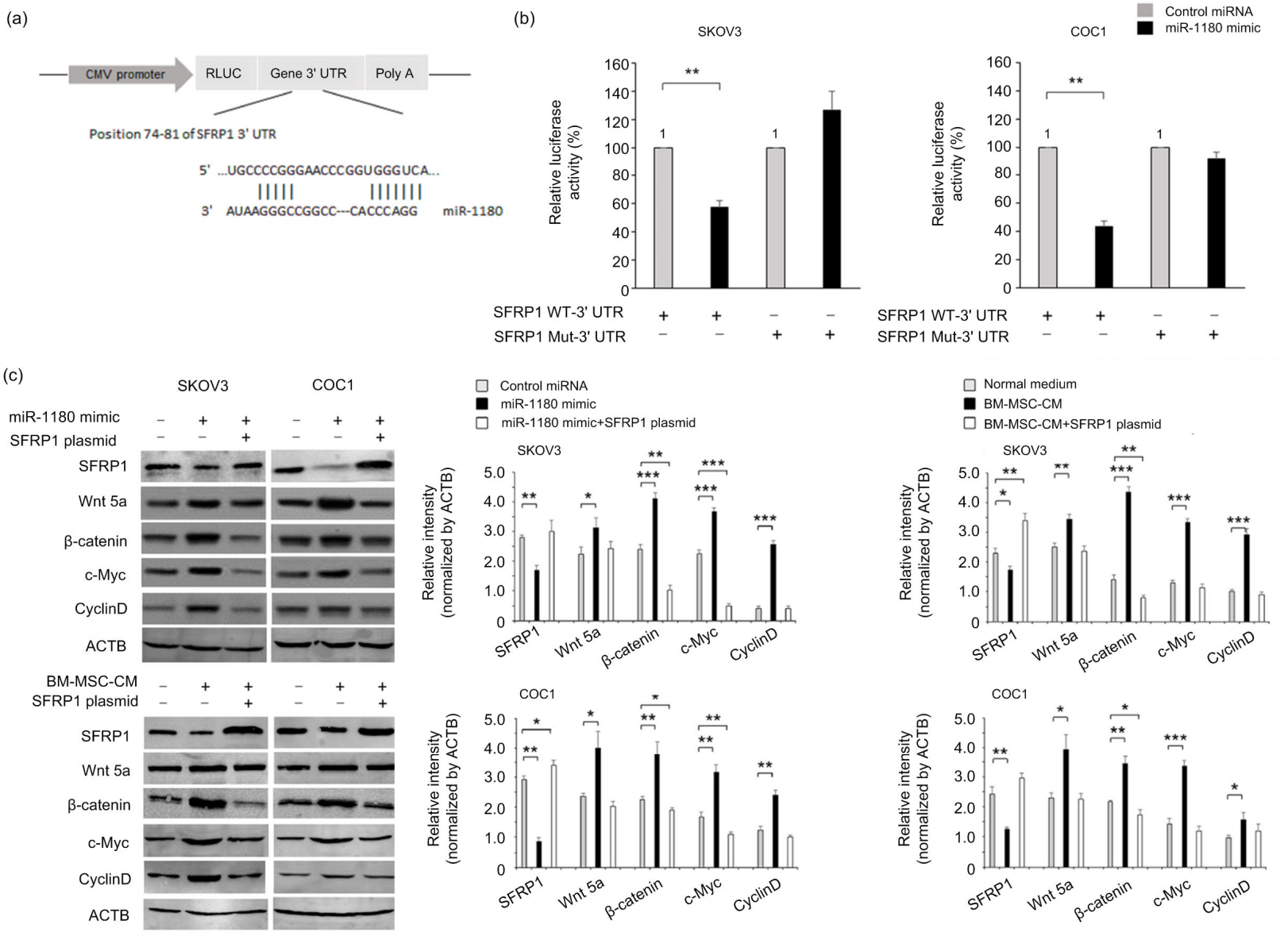
(a)
CMV promoter
RLUC
Gene 3' UTR
Poly A
Position 74-81 of SFRP1 3' UTR
5' ...UGCCCCGGGAACCCGGUGGGUCA...
3' AUAAGGGCCGGCC---CACCCAGG
miR-1180
(b)
SKOV3
COC1
Control miRNA
miR-1180 mimic
Relative luciferase activity (%)
SFRP1 WT-3' UTR
SFRP1 Mut-3' UTR
(c)
SKOV3
COC1
miR-1180 mimic
SFRP1 plasmid
BM-MSC-CM
SFRP1
Wnt 5a
β-catenin
c-Myc
CyclinD
ACTB
Control miRNA
miR-1180 mimic
miR-1180 mimic+SFRP1 plasmid
Normal medium
BM-MSC-CM
BM-MSC-CM+SFRP1 plasmid
Relative intensity (normalized by ACTB)

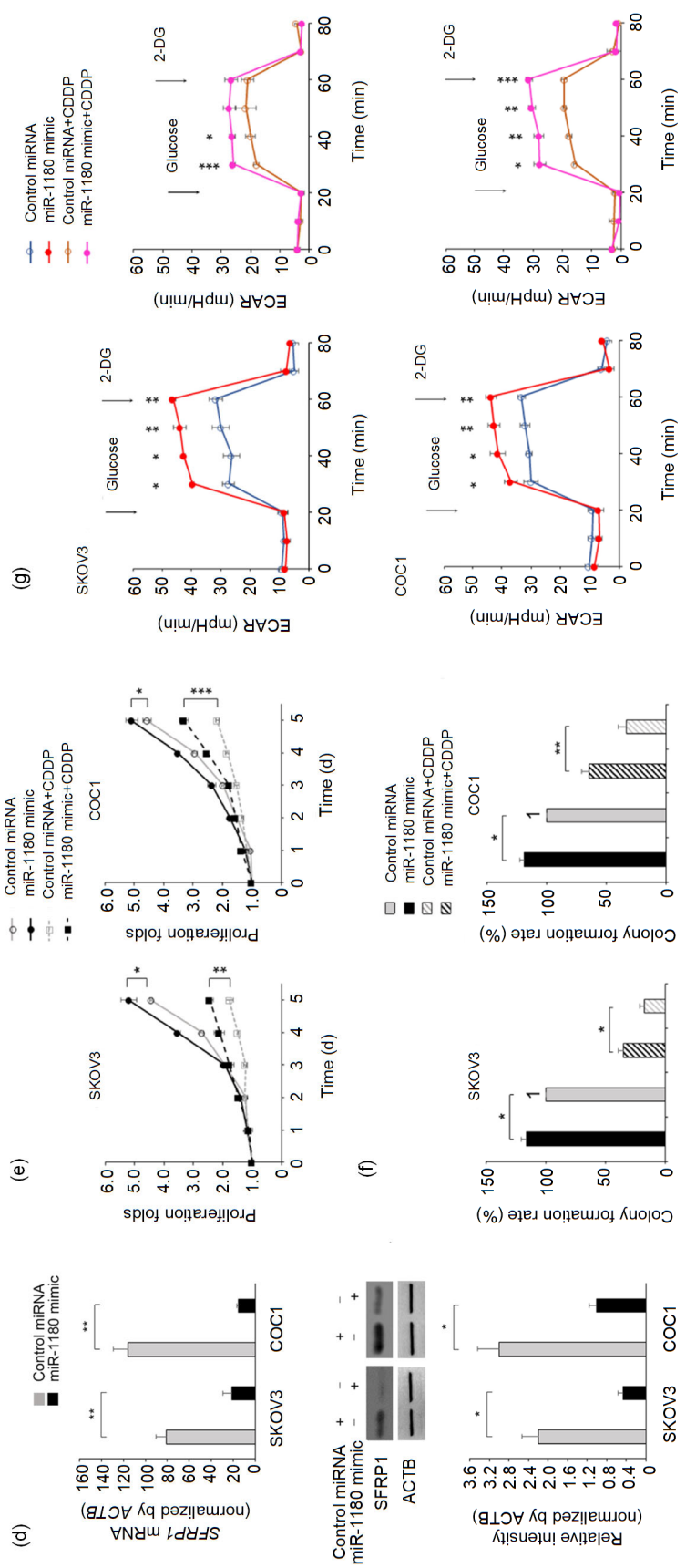

Fig. 5 Activation of miR-1180 on the Wnt signaling pathway by targeting SFRP1

(a) Schematic presentation of the luciferase reporter plasmid harboring a 3′ UTR sequence of SFRP1. (b) Comparisons of luciferase activity in cells transfected with an SFRP1 WT-3′ UTR or an SFRP1 Mut-3′ UTR plasmid in normal or miR-1180-deprived BM-MSC-CM. (c) Western blotting analysis of downstream components of the Wnt signaling pathway in cells treated with negative control, miR-1180 mimic, normal medium or BM-MSC-CM, with or without an SFRP1-expressing plasmid. (d) The mRNA and protein expression levels of SFRP1 in the cells treated with a negative control or a miR-1180 mimic. (e) Proliferative curves and (f) colony formation rates for control microRNA- or miR-1180 mimic-treated cells under a normal or a cisplatin-containing culture condition (0.5 mg/L). (g) The ECARs of control microRNA- or miR-1180 mimic-treated cells under a normal or a cisplatin-containing condition (0.5 mg/L). Glucose and 2-DG were added to start or stop, respectively, the intracellular glycolytic process of the cells. * $P<0.05$, ** $P<0.01$, *** $P<0.001$, two-sided Student's t-test. Data are expressed as mean±standard deviation (SD)

4.1 times higher than that of normal tissues, and the difference was statistically significant (Fig. 6b). The median T-N value was 5.1 among the enrolled patients. To confirm that the detected miR-1180 molecules were derived mainly from the infiltrating BM-MSCs and not from the cancer cells, we isolated BM-MSCs from cancer tissue with a CD271-based FACS technique. A parallel CD271 IHC-staining procedure was performed to verify the existence of BM-MSCs within cancer tissue. Meanwhile, cancer cells were isolated by EpCAM-based FACS. $CD271^+$ BM-MSCs were observed in 86% (51/59) of the specimens examined, suggesting that migration of BM-MSCs into cancer tissue is a frequent event in the patient body. Of these cases, the average miR-1180 level per cell in intra-tumoral BM-MSCs was significantly higher (by 3.2 times) than that of cancer cells (Fig. 6c). Moreover, BM-MSCs that expressed an increased level (i.e. higher than baseline level of normal tissue) of precursor molecule of miR-1180 (defined as "pre-miR-1180-expressing BM-MSCs") were detected in 76% (39/51) of intra-tumoral BM-MSC-positive cases. The average level of pre-miR-1180 per cell measured in these BM-MSCs was 48.4 times higher than that of FACS-sorted cancer cells from the same specimens, suggesting that BM-MSCs were a major source of miR-1180 in these cases (Fig. 6e). This type of pre-miR-1180-expressing BM-MSC was found in 97% (28/29) of cases in the high-miR-1180 group (T-N value>median) but in only 37% (11/30) of cases in the low-miR-1180 group (T-N value≤median). The difference was statistically significant (Fig. 6f).

Kaplan-Meier analysis revealed that the long-term (96 months) overall survival of ovarian cancer patients was significantly shorter in the high-miR-1180 group than in the low-miR-1180 group (Fig. 6g). In multivariate analysis, the overexpression of miR-1180 (T-N value>median) was further demonstrated to be an independent determinant of a poor outcome for the enrolled patients (Table 1). Moreover, of the 59 enrolled patients, 37 experienced chemoresistant recurrence during their follow-up periods. Of those, 73% (27/37) had a higher level of miR-1180 within their cancer tissue. This percentage was significantly higher than that detected in those without chemoresistant recurrence (9%; 2/22) (Table 2). Furthermore, the qPCR data indicated that the average miR-1180 level was significantly higher in patients with chemoresistant recurrence (Fig. 6h). The incidence rate of chemoresistant recurrence was 93% (27/29) in the high-miR-1180 group and 33% (10/30) in the low-miR-1180 group. This difference was statistically significant (Fig. 6i). Multivariate analysis revealed that overexpression of miR-1180 (T-N value>median) was also an independent prognostic factor for chemoresistant recurrence (Table 2). Additionally, as intra-tumoral miR-1180 and *SFRP1* mRNA levels were simultaneously measured for each specimen, the expression levels of these two molecules were found to be inversely correlated (Pearson's correlation coefficient r=0.804, P<0.05), revealing a negative regulatory effect of miR-1180 on the expression level of SFRP1 (Fig. 6j).

4 Discussion

The present study demonstrated the role of BM-MSC-derived microRNAs, especially miR-1180, in the occurrence of chemoresistance (mainly against cisplatin) in ovarian cancer. The in vitro data revealed that miR-1180-containing BM-MSC-CM can simultaneously strengthen glycolysis and chemoresistance in treated cancer cells (Figs. 4 and 5). Considering that glycolysis is an established intrinsic chemoresistance-promoting factor, we can interpret the observed chemoresistance enhancement as a consequence of miR-1180-induced glycolysis in the cancer cells (Figs. 1–5). The molecular mechanism by which miR-1180 induces glycolysis was also explored in our experiments (Figs. 5 and 6). The critical roles of the Wnt signaling pathway and its negative regulator, SFRP1, in mediating miR-1180-induced glycolysis were elucidated (Fig. 5); meanwhile, qPCR analysis of clinical specimens confirmed that SFRP1 is a major target of miR-1180 (Fig. 6). Most importantly, our population-based study revealed the clinical significance of miR-1180 as a prognostic factor for poor outcomes and as a predictor of chemoresistant recurrence in ovarian cancer patients (Fig. 6).

Multiple mechanisms by which BM-MSCs maintain cancer chemoresistance have been revealed by earlier studies. Cai et al. (2016) reported that BM-MSCs could induce glycolysis and chemoresistance in T-cell acute lymphoblastic leukemia via

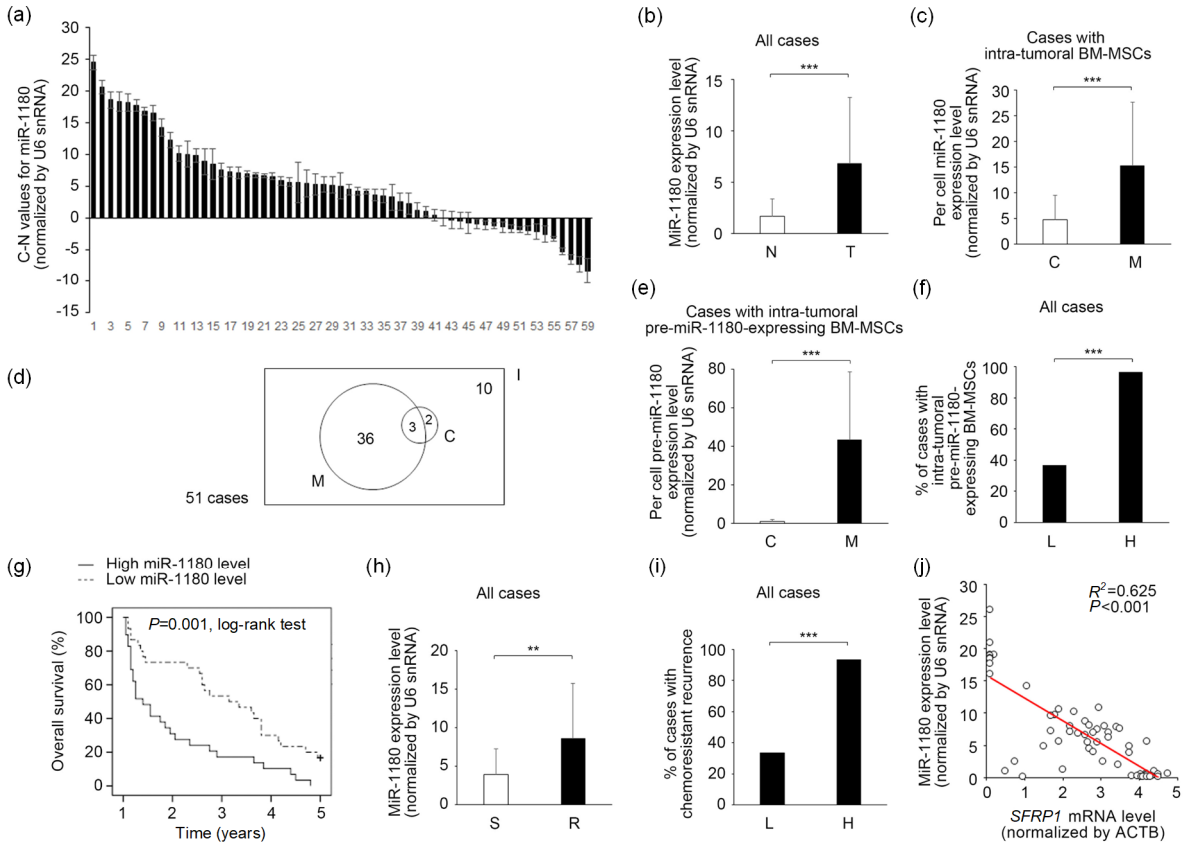

Fig. 6 Clinical significance of BM-MSC-CM-derived miR-1180 in ovarian cancer patients

(a) Ranking of the miR-1180 C-N values of enrolled patients' specimens. (b) Comparison of the miR-1180 levels between cancer tissue (T) and adjacent normal tissue (N) in all cases (59 cases). (c) Comparison of the per cell miR-1180 levels between BM-MSCs (M) and cancer cells (C) in cases with intra-tumoral BM-MSCs (51 cases). (d) A Venn diagram of the distributions of cases with pre-miR-1180-expressing BM-MSCs (with a pre-miR-1180 level higher than baseline level of normal tissue, 39 cases, M) and cases with pre-miR-1180-expressing cancer cells (5 cases, C) in cases with intra-tumoral BM-MSCs (51 cases, I). (e) Comparison of the per cell pre-miR-1180 levels between BM-MSCs (M) and cancer cells (C) in cases with intra-tumoral pre-miR-1180-expressing BM-MSCs (39 cases). (f) Distributions of the cases with intra-tumoral pre-miR-1180-expressing BM-MSCs in the high miR-1180 group (H) and in the low miR-1180 group (L). (g) Kaplan-Meier analysis of the overall survival of patients with either a higher or lower miR-1180 expression level. (h) Comparison of the miR-1180 levels of patients with (R) or without (S) chemoresistant recurrence. (i) Distributions of the cases with chemo-resistant recurrence in the high miR-1180 group (H) and in the low miR-1180 group (L). (j) Relationship of the intra-tumoral miR-1180 and *SFRP1* expression levels in enrolled patients' specimens. The expression statuses were inversely correlated. Two-sided Student's *t*-test (b, c, e, h), χ^2-test (f, i), log-rank test (g) or Pearson's product–moment correlation coefficient analysis (j) were adopted as appropriate. $^{*}P<0.05$, $^{**}P<0.01$, $^{***}P<0.001$. Data are expressed as mean±standard deviation (SD)

two strategies, i.e. soluble factor-mediated and cell adhesion-mediated pathways. Both BM-MSC-CM and direct contact with BM-MSCs can cause the dysfunction of mitochondria, and thereafter, reduce the production of ATP and reactive oxygen species (ROS). Consequently, an increased cytoplasmic lactate concentration and chemoresistance against cytosine arabinoside and methotrexate were achieved. However, Cai et al. (2016) did not explore the exact extracellular molecule responsible for transmitting glycolysis-regulatory signals from BM-MSCs to leukemia cells. Benabbou et al. (2014) reported that BM-MSCs can regulate the expression of ATP-binding cassette genes, e.g. multidrug resistance 1 (MDR1), multidrug resistance protein (MRP) 1/2/3, and breast cancer resistance protein (BCRP), in cancer cells by releasing insulin-like growth factor 1 (IGF1). Munoz et al. (2015) reported that miR-9 enhances the activity of the Sonic Hedgehog (SHH) pathway and chemoresistance of glioblastoma multiforme. They further

Table 1 Univariate and multivariate analyses of the clinico-pathological characteristics of the study population

Characteristics	Overall survival[#]			Multivariate analysis[##]		
	<8 years	≥8 years	*P* value	Hazard ratio	95% CI	*P* value
Age (years)			0.350			
<50	12 (22)	2 (40)				
50–59	22 (41)	0 (0)				
60–69	14 (26)	2 (40)				
≥70	6 (11)	1 (20)				
Gravidity			0.442			
0–1	7 (13)	1 (20)				
2–3	32 (59)	3 (60)				
4–5	12 (22)	0 (0)				
≥6	3 (6)	1 (20)				
Parity			0.564			
0–1	39 (72)	3 (60)				
2–3	15 (28)	2 (40)				
Ascites			0.493			
Yes	19 (35)	1 (20)				
No	35 (65)	4 (80)				
Lymphatic metastasis			0.008*			0.028*
Yes	33 (61)	0 (0)		1 (reference)		
No	21 (39)	5 (100)		2.116	(1.085, 4.124)	
Stage			<0.001*			0.037*
I	1 (2)	3 (60)		1 (reference)		
II	12 (22)	1 (20)		4.228	(0.505, 35.426)	
III	38 (70)	1 (20)		10.543	(1.225, 90.740)	
IV	3 (6)	0 (0)		13.039	(1.079, 157.581)	
Histotype			0.001*			0.007*
Serous	39 (72)	0 (0)		1 (reference)		
Mucinous	4 (8)	2 (40)		0.063	(0.006, 0.709)	
Endometrioid	5 (9)	3 (60)		0.016	(0.001, 0.221)	
Clear cell	5 (9)	0 (0)		0.027	(0.002, 0.347)	
Undifferentiated	1 (2)	0 (0)		0.093	(0.007, 1.310)	
Grade			0.032*			0.482
G1	14 (26)	4 (80)		1 (reference)		
G2	14 (26)	1 (20)		1.540	(0.681, 3.484)	
G3	26 (48)	0 (0)		1.552	(0.689, 3.492)	
Residual site			0.023*			0.015*
<1 cm	16 (30)	4 (80)		1 (reference)		
≥1 cm	38 (70)	1 (20)		3.031	(1.245, 7.380)	
Chemoresponse			0.039*			0.008*
Sensitive	18 (33)	4 (80)		1 (reference)		
Resistant	36 (67)	1 (20)		3.461	(1.393, 8.602)	
Intra-tumoral miR-1180 level			0.022*			0.027*
Low	25 (46)	5 (100)		1 (reference)		
High	29 (54)	0 (0)		2.831	(1.129, 7.100)	

* Statistical significance. # The overall survival rates are presented as number (percentage); χ^2-test was used for univariate analysis. ## The hazard ratio of the reference group was set as 1; Cox regression model was used for multivariate analysis. 95% CI: 95% confidence interval

Table 2 Univariate and multivariate analyses of the risk factors of chemoresistant recurrence

Characteristics	Chemoresistant recurrence[#]			Multivariate analysis[##]		
	Occurred	Not occurred	*P* value	Hazard ratio	95% CI	*P* value
Age (years)			0.540			
<50	9 (24)	5 (23)				
50–59	16 (43)	6 (27)				
60–69	8 (22)	8 (36)				
≥70	4 (11)	3 (14)				
Gravidity			0.082			
0–1	3 (8)	5 (23)				
2–3	26 (70)	9 (41)				
4–5	7 (19)	5 (23)				
≥6	1 (3)	3 (13)				
Parity			0.840			
0–1	26 (70)	16 (73)				
2–3	11 (30)	6 (27)				
Ascites			0.407			
Yes	14 (38)	6 (27)				
No	23 (62)	16 (73)				
Lymphatic metastasis			0.869			
Yes	21 (57)	12 (55)				
No	16 (43)	10 (45)				
Stage			0.279			
I	2 (6)	2 (9)				
II	6 (16)	7 (32)				
III	26 (70)	13 (59)				
IV	3 (8)	0 (0)				
Histotype			0.226			
Serous	28 (76)	11 (50)				
Mucinous	3 (8)	3 (14)				
Endometrioid	3 (8)	5 (23)				
Clear cell	2 (5)	3 (14)				
Undifferentiated	1 (3)	0 (0)				
Grade			0.341			
G1	10 (27)	8 (36)				
G2	8 (22)	7 (32)				
G3	19 (51)	7 (32)				
Residual site			0.002*			0.060
<1 cm	7 (19)	13 (59)		1 (reference)		
≥1 cm	30 (81)	8 (41)		2.590	(0.961, 6.981)	
Intra-tumoral miR-1180 level			<0.001*			<0.001*
Low	10 (27)	20 (81)		1 (reference)		
High	27 (73)	2 (9)		5.612	(2.388, 13.190)	

* Statistical significance. # The chemoresistant recurrence rates are presented as number (percentage); χ^2-test was used for univariate analysis. ## The hazard ratio of the reference group was set as 1; Cox regression model was used for multivariate analysis. 95% CI: 95% confidence interval

suggested that BM-MSCs can be used to deliver anti-miR-9 into the brain and transfer this molecule to tumor cells through an exosome-based approach. Likewise, our current study showed that BM-MSCs apply a microRNA-mediated remote communication mechanism, possibly involving exosome-based transportation, and induce glycolysis and chemoresistance in ovarian cancer cells.

The Wnt signaling pathway has been found to be involved in a series of intrinsic mechanisms to induce the chemoresistance of ovarian cancer. The key downstream proteins (genes) activated by Wnt/β-catenin signaling include c-Myc, CyclinD1 (CCND1), Survivin (BIRC5), and Axin2 (i.e. "stemness/proliferation" related genes), which strengthen the potential of cancer cells for proliferation, survival, and metastasis under chemotherapeutic pressure (Barbolina et al., 2011). Wnt/β-catenin signaling also plays an important role in the transcriptional control of multidrug resistance genes such as *MDR-1* (Takahashi-Yanaga and Kahn, 2010). Moreover, activation of the Wnt signaling pathway can result in the upregulation of a group of epithelial to mesenchymal transition (EMT)-related genes, e.g. *MMP9*, *PTGS2* (*COX2*), *PLAUR* (*uPAR*), *Vimentin* (*VIM*), and *SNAIL* (*SNAI1*), at the mRNA level (Burkhalter et al., 2011). EMT itself is a promotive cytological factor for chemoresistance (Latifi et al., 2011; Abubaker et al., 2013). Pate et al. (2014) indicated that Wnt signaling can initiate a critical change in tumorigenesis, namely Warburg metabolism or aerobic glycolysis (Warburg, 1956), through the activation of transcription of a downstream effector, pyruvate dehydrogenase kinase 1 (PDK1). Herein, our experiments demonstrated that Wnt signaling-induced glycolysis is a critical factor contributing to the chemoresistant recurrence of ovarian cancer, which has not been identified before (Figs. 4 and 5). Also, supplementation of SFRP1 was found to be an effective measure to quench the glycolysis induced by the activated Wnt pathway in an miR-1180-containing microenvironment (Fig. 5).

MiR-1180 was recognized as an onco-miR in solid cancers including hepatocellular carcinoma, pancreatic cancer, and lung cancer (Tan et al., 2016; Zhou et al., 2016; Chen et al., 2017; Gu et al., 2017). With respect to the detailed roles of miR-1180, Zhou et al. (2016) indicated that miR-1180 can downregulate the TNFAIP3 interacting protein 2 (TNIP2), an essential negative regulator of the nuclear factor-κB (NF-κB) pathway, and enhance the proliferation of hepatic cancer cells. Similarly, Gu et al. (2017) reported that miR-1180 can stimulate the proliferation and metastasis of pancreatic cancer cells through an NF-κB-signaling-related mechanism. Chen et al. (2017) reported that miR-1180 can simultaneously enhance two signaling pathways, i.e. Wnt/β-catenin and PI3K/Akt, to upregulate proliferation, migration, and invasion activities in lung cancer cells. Tan et al. (2016) asserted that miR-1180 can promote chemoresistance by targeting two key inhibitors in the NF-κB pathway in hepatocellular carcinoma, i.e. OTU deubiquitinase 7B (OTUD7B) and TNIP2. All these authors reported that an increase in miR-1180 was a prognostic factor for poor outcomes for patients. However, other studies found evidence to the contrary. For example, Zhu et al. (2018) showed that miR-1180 expression was reduced in prostate cancer tissues and overexpression of miR-1180 could inhibit proliferation, migration, and invasion, and promote the apoptosis of the prostate cancer cell line DU145 by targeting TNF receptor associated factor 1 (TRAF1) and BCL2-associated athanogene 2 (BAG2). Similarly, Wang et al. (2014) and Ge et al. (2017) observed that miR-1180 can induce the expression of p21 and inhibit the cell cycle-related proteins CDK4, CDK6, CyclinD1, and CyclinA2, and suppress the growth of bladder cancer cells in vitro and in vivo. Clearly, our data, obtained from ovarian cancer, support miR-1180 as a pro-tumoral factor for the chemoresistance and recurrence of cancer.

In conclusion, our experiments confirmed that BM-MSC-derived miR-1180 is associated with increased glycolysis and chemoresistance in ovarian cancer. The suppression of miR-1180 expression with an antisense microRNA can induce chemosensitivity to genotoxic agents, such as cisplatin. Therefore, miR-1180 may be a potential therapeutic target for reversing "Warburg effect"-induced chemoresistance and improving the long-term survival of patients (Ganapathy-Kanniappan and Geschwind, 2013; Suh et al., 2014; Icard et al., 2018; Yao ZY et al., 2018).

Contributors

Zhuo-wei GU, Wen-jing WANG, and Qi TIAN performed the in vitro experiments. Zhuo-wei GU and Yi-feng HE collected the medical records of the enrolled patients. Yi-feng HE analyzed the data and wrote the manuscript. Yi-feng HE

and Wen DI designed the study. All authors read and approved the final manuscript and, therefore, had full access to all the data in the study and take responsibility for the integrity and security of the data.

Compliance with ethics guidelines

Zhuo-wei GU, Yi-feng HE, Wen-jing WANG, Qi TIAN, and Wen DI declare that they have no conflict of interest.

All procedures followed were in accordance with the ethical standards of the responsible committee on human experimentation (institutional and national) and with the Helsinki Declaration of 1975, as revised in 2008 (5). Informed consent was obtained from all patients for being included in the study.

References

Abubaker K, Latifi A, Luwor R, et al., 2013. Short-term single treatment of chemotherapy results in the enrichment of ovarian cancer stem cell-like cells leading to an increased tumor burden. *Mol Cancer*, 12:24. https://doi.org/10.1186/1476-4598-12-24

Arend RC, Londoño-Joshi AI, Straughn JM Jr, et al., 2013. The Wnt/β-catenin pathway in ovarian cancer: a review. *Gynecol Oncol*, 131(3):772-779. https://doi.org/10.1016/j.ygyno.2013.09.034

Barbolina MV, Burkhalter RJ, Stack MS, 2011. Diverse mechanisms for activation of Wnt signalling in the ovarian tumour microenvironment. *Biochem J*, 437(1):1-12. https://doi.org/10.1042/BJ20110112

Benabbou N, Mirshahi P, Bordu C, et al., 2014. A subset of bone marrow stromal cells regulate ATP-binding cassette gene expression via insulin-like growth factor-I in a leukemia cell line. *Int J Oncol*, 45(4):1372-1380. https://doi.org/10.3892/ijo.2014.2569

Burkhalter RJ, Symowicz J, Hudson LG, et al., 2011. Integrin regulation of β-catenin signaling in ovarian carcinoma. *J Biol Chem*, 286(26):23467-23475. https://doi.org/10.1074/jbc.M110.199539

Cai JY, Wang JC, Huang YN, et al., 2016. ERK/Drp1-dependent mitochondrial fission is involved in the MSC-induced drug resistance of T-cell acute lymphoblastic leukemia cells. *Cell Death Dis*, 7(11):e2459. https://doi.org/10.1038/cddis.2016.370

Castells M, Milhas D, Gandy C, et al., 2013. Microenvironment mesenchymal cells protect ovarian cancer cell lines from apoptosis by inhibiting XIAP inactivation. *Cell Death Dis*, 4(10):e887. https://doi.org/10.1038/cddis.2013.384

Chen EG, Zhang JS, Xu S, et al., 2017. Long non-coding RNA DGCR5 is involved in the regulation of proliferation, migration and invasion of lung cancer by targeting miR-1180. *Am J Cancer Res*, 7(7):1463-1475.

Coffman LG, Choi YJ, McLean K, et al., 2016. Human carcinoma-associated mesenchymal stem cells promote ovarian cancer chemotherapy resistance via a BMP4/HH signaling loop. *Oncotarget*, 7(6):6916-6932. https://doi.org/10.18632/oncotarget.6870

Das B, Kashino SS, Pulu I, et al., 2013. $CD271^+$ bone marrow mesenchymal stem cells may provide a niche for dormant *Mycobacterium tuberculosis*. *Sci Transl Med*, 5(170):170ra13. https://doi.org/10.1126/scitranslmed.3004912

Fu DL, Jiang QH, He FM, et al., 2017. Adhesion of bone marrow mesenchymal stem cells on porous titanium surfaces with strontium-doped hydroxyapatite coating. *J Zhejiang Univ-Sci B (Biomed & Biotechnol)*, 18(9):778-788. https://doi.org/10.1631/jzus.B1600517

Ganapathy-Kanniappan S, Geschwind JF, 2013. Tumor glycolysis as a target for cancer therapy: progress and prospects. *Mol Cancer*, 12:152. https://doi.org/10.1186/1476-4598-12-152

Ge QQ, Wang CH, Chen Z, et al., 2017. The suppressive effects of miR-1180-5p on the proliferation and tumorigenicity of bladder cancer cells. *Histol Histopathol*, 32(1):77-86. https://doi.org/10.14670/HH-11-772

Gu L, Zhang JQ, Shi MM, et al., 2017. The effects of miRNA-1180 on suppression of pancreatic cancer. *Am J Transl Res*, 9(6):2798-2806.

He YF, Zhu QJ, Chen M, et al., 2016. The changing 50% inhibitory concentration (IC_{50}) of cisplatin: a pilot study on the artifacts of the MTT assay and the precise measurement of density-dependent chemoresistance in ovarian cancer. *Oncotarget*, 7(43):70803-70821. https://doi.org/10.18632/oncotarget.12223

Huang RX, Wu D, Yuan Y, et al., 2014. CD117 expression in fibroblasts-like stromal cells indicates unfavorable clinical outcomes in ovarian carcinoma patients. *PLoS ONE*, 9(11):e112209. https://doi.org/10.1371/journal.pone.0112209

Icard P, Shulman S, Farhat D, et al., 2018. How the Warburg effect supports aggressiveness and drug resistance of cancer cells? *Drug Resist Updat*, 38:1-11. https://doi.org/10.1016/j.drup.2018.03.001

Jones EA, Crawford A, English A, et al., 2008. Synovial fluid mesenchymal stem cells in health and early osteoarthritis: detection and functional evaluation at the single-cell level. *Arthritis Rheum*, 58(6):1731-1740. https://doi.org/10.1002/art.23485

Latifi A, Abubaker K, Castrechini N, et al., 2011. Cisplatin treatment of primary and metastatic epithelial ovarian carcinomas generates residual cells with mesenchymal stem cell-like profile. *J Cell Biochem*, 112(10):2850-2864. https://doi.org/10.1002/jcb.23199

Lis R, Touboul C, Mirshahi P, et al., 2011. Tumor associated mesenchymal stem cells protects ovarian cancer cells from hyperthermia through CXCL12. *Int J Cancer*, 128(3):715-725. https://doi.org/10.1002/ijc.25619

Lis R, Touboul C, Halabi NM, et al., 2014. Mesenchymal cell interaction with ovarian cancer cells induces a background

dependent pro-metastatic transcriptomic profile. *J Transl Med*, 12:59. https://doi.org/10.1186/1479-5876-12-59

Mader EK, Maeyama Y, Lin Y, et al., 2009. Mesenchymal stem cell carriers protect oncolytic measles viruses from antibody neutralization in an orthotopic ovarian cancer therapy model. *Clin Cancer Res*, 15(23):7246-7255. https://doi.org/10.1158/1078-0432.CCR-09-1292

McLean K, Gong YS, Choi Y, et al., 2011. Human ovarian carcinoma-associated mesenchymal stem cells regulate cancer stem cells and tumorigenesis via altered BMP production. *J Clin Invest*, 121(8):3206-3219. https://doi.org/10.1172/JCI45273

Munoz JL, Rodriguez-Cruz V, Walker ND, et al., 2015. Temozolomide resistance and tumor recurrence: halting the Hedgehog. *Cancer Cell Microenviron*, 2(2):e747. https://doi.org/10.14800/ccm.747

Noort WA, Oerlemans MIFJ, Rozemuller H, et al., 2012. Human *versus* porcine mesenchymal stromal cells: phenotype, differentiation potential, immunomodulation and cardiac improvement after transplantation. *J Cell Mol Med*, 16(8):1827-1839. https://doi.org/10.1111/j.1582-4934.2011.01455.x

Pate KT, Stringari C, Sprowl-Tanio S, et al., 2014. Wnt signaling directs a metabolic program of glycolysis and angiogenesis in colon cancer. *EMBO J*, 33(13):1454-1473. https://doi.org/10.15252/embj.201488598

Quirici N, Soligo D, Bossolasco P, et al., 2002. Isolation of bone marrow mesenchymal stem cells by anti-nerve growth factor receptor antibodies. *Exp Hematol*, 30(7): 783-791. https://doi.org/10.1016/S0301-472X(02)00812-3

Rasini V, Dominici M, Kluba T, et al., 2013. Mesenchymal stromal/stem cells markers in the human bone marrow. *Cytotherapy*, 15(3):292-306. https://doi.org/10.1016/j.jcyt.2012.11.009

Ridge SM, Sullivan FJ, Glynn SA, 2017. Mesenchymal stem cells: key players in cancer progression. *Mol Cancer*, 16:31. https://doi.org/10.1186/s12943-017-0597-8

Suh DH, Kim HS, Kim B, et al., 2014. Metabolic orchestration between cancer cells and tumor microenvironment as a co-evolutionary source of chemoresistance in ovarian cancer: a therapeutic implication. *Biochem Pharmacol*, 92(1):43-54. https://doi.org/10.1016/j.bcp.2014.08.011

Takahashi-Yanaga F, Kahn M, 2010. Targeting Wnt signaling: can we safely eradicate cancer stem cells? *Clin Cancer Res*, 16(12):3153-3162. https://doi.org/10.1158/1078-0432.CCR-09-2943

Tan GS, Wu LW, Tan JF, et al., 2016. MiR-1180 promotes apoptotic resistance to human hepatocellular carcinoma via activation of NF-κB signaling pathway. *Sci Rep*, 6: 22328. https://doi.org/10.1038/srep22328

Touboul C, Lis R, al Farsi H, et al., 2013. Mesenchymal stem cells enhance ovarian cancer cell infiltration through IL6 secretion in an amniochorionic membrane based 3D model. *J Transl Med*, 11:28. https://doi.org/10.1186/1479-5876-11-28

Touboul C, Vidal F, Pasquier J, et al., 2014. Role of mesenchymal cells in the natural history of ovarian cancer: a review. *J Transl Med*, 12:271. https://doi.org/10.1186/s12967-014-0271-5

Tyciakova S, Matuskova M, Bohovic R, et al., 2015. Genetically engineered mesenchymal stromal cells producing TNFα have tumour suppressing effect on human melanoma xenograft. *J Gene Med*, 17(1-2):54-67. https://doi.org/10.1002/jgm.2823

Vallabhaneni KC, Hassler MY, Abraham A, et al., 2016. Mesenchymal stem/stromal cells under stress increase osteosarcoma migration and apoptosis resistance via extracellular vesicle mediated communication. *PLoS ONE*, 11(11):e0166027. https://doi.org/10.1371/journal.pone.0166027

Wang CH, Chen Z, Ge QQ, et al., 2014. Up-regulation of $p21^{WAF1/CIP1}$ by miRNAs and its implications in bladder cancer cells. *FEBS Lett*, 588(24):4654-4664. https://doi.org/10.1016/j.febslet.2014.10.037

Wang WW, Zhong W, Yuan JH, et al., 2015. Involvement of Wnt/β-catenin signaling in the mesenchymal stem cells promote metastatic growth and chemoresistance of cholangiocarcinoma. *Oncotarget*, 6(39):42276-42289. https://doi.org/10.18632/oncotarget.5514

Warburg O, 1956. On the origin of cancer cells. *Science*, 123(3191):309-314. https://doi.org/10.1126/science.123.3191.309

Watson JT, Foo T, Wu J, et al., 2013. CD271 as a marker for mesenchymal stem cells in bone marrow versus umbilical cord blood. *Cells Tissues Organs*, 197(6):496-504. https://doi.org/10.1159/000348794

Watts TL, Cui RW, Szaniszlo P, et al., 2016. PDGF-AA mediates mesenchymal stromal cell chemotaxis to the head and neck squamous cell carcinoma tumor microenvironment. *J Transl Med*, 14(1):337. https://doi.org/10.1186/s12967-016-1091-6

Wu H, Ding ZH, Hu DQ, et al., 2012. Central role of lactic acidosis in cancer cell resistance to glucose deprivation-induced cell death. *J Pathol*, 227(2):189-199. https://doi.org/10.1002/path.3978

Wu M, Neilson A, Swift AL, et al., 2007. Multiparameter metabolic analysis reveals a close link between attenuated mitochondrial bioenergetic function and enhanced glycolysis dependency in human tumor cells. *Am J Physiol Cell Physiol*, 292(1):C125-C136. https://doi.org/10.1152/ajpcell.00247.2006

Xiang BY, Chen L, Wang XJ, et al., 2017. Mesenchymal stem cells as therapeutic agents and in gene delivery for the treatment of glioma. *J Zhejiang Univ-Sci B (Biomed & Biotechnol)*, 18(9):737-746.

https://doi.org/10.1631/jzus.B1600337

Yang YY, Otte A, Hass R, 2015. Human mesenchymal stroma/stem cells exchange membrane proteins and alter functionality during interaction with different tumor cell lines. *Stem Cells Dev*, 24(10):1205-1222. https://doi.org/10.1089/scd.2014.0413

Yao K, Fu XF, Du X, et al., 2018. PGC-1α coordinates with Bcl-2 to control the cell cycle in U251 cells through reducing ROS. *J Zhejiang Univ-Sci B (Biomed & Biotechnol)*, 19(6):415-424. https://doi.org/10.1631/jzus.B1700148

Yao ZY, Chen WB, Shao SS, et al., 2018. Role of exosome-associated microRNA in diagnostic and therapeutic applications to metabolic disorders. *J Zhejiang Univ-Sci B (Biomed & Biotechnol)*, 19(3):183-198. https://doi.org/10.1631/jzus.B1600490

Zhang MY, He YF, Sun XJ, et al., 2014. A high M1/M2 ratio of tumor-associated macrophages is associated with extended survival in ovarian cancer patients. *J Ovarian Res*, 7:19. https://doi.org/10.1186/1757-2215-7-19

Zhou X, Zhu HQ, Ma CQ, et al., 2016. MiR-1180 promoted the proliferation of hepatocellular carcinoma cells by repressing TNIP2 expression. *Biomed Pharmacother*, 79:315-320. https://doi.org/10.1016/j.biopha.2016.02.025

Zhu DY, Gao WX, Zhang ZM, 2018. MicroRNA-1180 is associated with growth and apoptosis in prostate cancer via TNF receptor associated factor 1 expression regulation and nuclear factor-κB signaling pathway activation. *Oncol Lett*, 15(4):4775-4780. https://doi.org/10.3892/ol.2018.7914

中文概要

题　目：骨髓间充质干细胞释放 miR-1180 上调 Wnt 信号通路活性并促进卵巢癌细胞糖酵解和化疗耐药能力的研究

目　的：已知骨髓间充质干细胞在癌症的发生发展中起有重要作用，本研究分析它们在增强卵巢癌化疗耐药能力中的具体作用。

创新点：发现骨髓间充质干细胞可以通过释放微小 RNA（microRNA）影响卵巢癌化疗耐药能力，并确定了介导此作用的 microRNA 分子和相关作用机制。

方　法：收集骨髓间充质干细胞条件培养基，以微阵列方法分析其中 microRNA 表达谱。针对所获高表达 microRNA，分析它（们）对细胞内糖酵解及相关化疗耐药行为的影响。通过生物信息学方法查找所获 microRNA 的靶基因，分析信号作用机制。纳入 59 名卵巢癌患者，以 Kaplan-Merier 生存分析方法考察所获 microRNA 分子表达程度的临床预后意义。

结　论：迁移至卵巢癌组织内的骨髓间充质干细胞可释放 miR-1180 分子。MiR-1180 分子进入癌细胞后，识别并下调 SFRP1 蛋白（分泌型 Wnt 受体，起信号抑制作用），由此提高 Wnt 通路活性。活化后的 Wnt 信号通路可增强癌细胞内糖酵解水平（即 Warburg 效应），从而引起糖酵解依赖性化疗耐药行为。

关键词：卵巢癌化疗耐药；间充质干细胞；MiR-1180；SFRP1；Wnt；糖酵解